Heterogeneous DNA Adduct Formation in Vitro by the Acetylated Food Mutagen 2-(Acetoxyamino)-1-methyl-6-phenylimidazo[4,5-*b*]pyridine: A Fluorescence Spectroscopic Study

Glenn A. Marsch, Eli N. Goldman, Esther Fultz, Nancy H. Shen, and Kenneth W. Turteltaub*

Biology and Biotechnology Research Program, L-452, Lawrence Livermore National Laboratory, Livermore, California 94551

Received January 30, 1995®

The food mutagen 2-amino-1-methyl-6-phenylimidazo[4,5-*b*]pyridine (PhIP) forms adducts to DNA guanine bases at the C-8 position. No other DNA adduction site has been verified for PhIP, nor has any experimental data been collected on the conformation of the PhIP-DNA covalent complex. To determine if multiple PhIP-DNA adduct species exist, or if PhIP-DNA adducts assume multiple conformations, 2-(acetoxyamino)-1-methyl-6-phenylimidazo[4,5-*b*]-pyridine (*N*-acetoxy-PhIP) was reacted with calf thymus DNA, followed by an evaluation of the resulting adduct complexes by fluorescence spectroscopy. Approximately 20% of the *N*-acetoxy-PhIP formed covalent complexes with DNA. Two major and several minor spots were observed by ^{32}P-postlabeling, suggesting a minimum of two major adduct species. UV/vis spectra of the PhIP-modified DNA also showed heterogeneous formation of PhIP-DNA adducts. Fluorescence excitation and emission spectroscopy with or without fluorescence quenching (silver ion and acrylamide) was used to evaluate the number of adducts formed, and the low-resolution conformation of each adduct. Four adduct fluorophores were observed and assigned the nomenclature PA*i*, where "PA" denotes PhIP Adduct and $i = 1-4$ in order of fluorescence emission band energies, with 1 the highest and 4 the lowest energy, respectively. Excitation maxima for the adduct fluorophores ranged from 340 to 370 nm, and emission maxima ranged from 390 to 420 nm. The fluorescence from adduct PA1 was quenched by silver but not acrylamide, suggesting a helix-internal configuration. Adduct PA2 fluorescence was strongly enhanced upon silver binding but was not affected by acrylamide, also indicating that this adduct was internal. The fluorescence from adducts PA3 and PA4 was quenched by acrylamide but not silver; thus PA2 and PA3 were tentatively assigned as solvent-accessible. These data are the first suggesting heterogeneous formation of PhIP adducts to intact DNA, but we cannot as yet determine how many chemical species of adduct are formed or if a given species exists in multiple conformations.

Introduction

Heterocyclic amines have been intensely studied for their role in mutagenesis and carcinogenesis. Some heterocyclic amines are widely distributed in foodstuffs consumed in the Western diet (*1–3*), but are found in especially high concentrations in muscle meats cooked at high temperatures (*4–7*). Of the food-borne heterocyclic amine mutagens, 2-amino-1-methyl-6-phenylimidazo[4,5-*b*]pyridine (PhIP)[1] is usually the most abundant (*6, 8*). PhIP is modestly mutagenic, inducing up to 2000 revertants/μg of PhIP in the Ames *Salmonella typhimurium* assay (*1, 6, 9*), but it is a potent carcinogen in rats and mice, causing breast and colon tumors in the former (*10, 11*) and lymphomas in the latter (*11, 12*). Thus the evidence suggests a possible role for PhIP in the etiology of human cancers.

PhIP is a hydrophobic procarcinogen that is inactive *per se*, but is metabolized in vivo to highly reactive electrophiles, including *N*-acetoxy-PhIP, that bind covalently to DNA (*13–18*). Although the ^{32}P-postlabeling assay suggests that at least two major adducts are formed in vivo by PhIP, all these adducts are to guanine bases (*19*), with adducts to poly(dA) and poly(dC) possibly being formed in very low yields (*20*). The predominant PhIP adduct, and indeed the only one so far identified, is the N^2-(2′-deoxyguanosin-8-yl)-PhIP (dG-C8-PhIP) adduct (*21–23*). However, two heterocyclic amine congeners, 2-amino-3,8-dimethylimidazo[4,5-*f*]quinoxaline (MeIQx) and 2-amino-3-methylimidazo[4,5-*f*]quinoline (IQ), are known to form covalent lesions through the N^2-exocyclic amine of guanines as well (*24, 25*).

To date, no experimental evidence has revealed the conformation of the covalent PhIP-DNA complex, or the existence of PhIP lesions at sites other than the C8 guanine position. However, recently molecular mechanics computations were undertaken on a theoretical model in which PhIP was covalently bound to a duplex DNA oligomer through a C8 guanine linkage. Using potential energy minimization searches, conformational modeling

* To whom correspondence should be addressed.

® Abstract published in *Advance ACS Abstracts,* May 1, 1995.

[1] Abbreviations: 2-(acetoxyamino)-1-methyl-6-phenylimidazo[4,5-*b*]-pyridine, *N*-acetoxy-PhIP; 2-amino-3,8-dimethylimidazo[4,5-*f*]quinoxaline, MeIQx; 2-amino-3-methylimidazo[4,5-*f*]quinoline, IQ; 2-amino-1-methyl-6-phenylimidazo[4,5-*b*]pyridine, PhIP; base pairs, bp; benzo[*a*]-pyrene diol epoxide, BPDE; emission wavelength, λ_{em}; energy gap between chromophore absorption and fluorescence maxima, ΔE; excitation wavelength, λ_{ex}; full width at half-maximum, FWHM; 2-(hydroxyamino)-1-methyl-6-phenylimidazo[4,5-*b*]pyridine, *N*-OH-PhIP; 3-(*N*-morpholino)propanesulfonic acid, MOPS; N^2-(2′-deoxyguanosin-8-yl)-PhIP, dG-C8-PhIP.

0893-228x/95/2708-0659$09.00/0

of the PhIP moiety led to a lowest energy conformation where the PhIP chromophore is tightly buried in the minor groove of the B-DNA helix (*26*).

In order to ascertain how many possible PhIP adducts may form, we undertook a fluorescence spectroscopic study of PhIP macromolecular adducts formed in vitro when *N*-acetoxy-PhIP was reacted with calf thymus DNA. A high molecular weight, random-sequence DNA was chosen to ensure that any PhIP adduct formed at fairly high efficiencies, but in a sequence-specific manner, would be detected. Covalent binding studies using defined-sequence oligodeoxynucleotides are better defined in one sense, but may not result in the adduct distribution found in genomic DNA. Thus, biologically deleterious PhIP adducts may not form to a given DNA oligomer sequence, but binding studies with random-sequence DNA provide a "benchmark", where all potential DNA binding sites are represented. We find that *N*-acetoxy-PhIP forms at least four distinguishable species of adduct fluorophore upon adduction to macromolecular DNA. Our findings also represent the first experimental evidence concerning the fluorescence properties of PhIP-DNA covalent complexes, leading to a preliminary assignment of PhIP adduct conformation at a low-resolution level. It is as yet unclear whether some of these adducts are due to linkage to a guanine nucleophilic center other than the C8.

Materials and Methods

Materials. Caution: *2-(Hydroxyamino)-1-methyl-6-phenylimidazo[4,5-b]pyridine (N-OH-PhIP) and its derivative N-acetoxy-PhIP are potential human carcinogens and should be handled carefully according to appropriate Environmental Safety and Health protocols.* *N*-OH-PhIP was purchased from SRI International (Palo Alto, CA), and calf thymus DNA was purchased from Sigma Chemical Co. (St. Louis, MO).

Activation of *N*-OH-PhIP to *N*-Acetoxy-PhIP. The *N*-OH-PhIP used in this study had a purity of >97% as measured by HPLC and thus was used without further purification. Briefly, *N*-OH-PhIP was *N*-O-acetylated according to a slight modification of previous protocols (*21–23*). Solutions were purged with anhydrous nitrogen gas and stirred during the entire course of the reaction. A 120× molar excess of glacial acetic acid was added to *N*-OH-PhIP in methanol (usually 0.3–0.5 mg/mL) at 0 °C, immediately followed by the addition, at 2.5 min intervals, of four aliquots (35× molar excess each aliquot) of 97% acetic anhydride (J. T. Baker, Inc.; Phillipsburg, NJ). After the final addition of acetic anhydride, the reaction was incubated 10 min longer on ice. The efficiency of activation to *N*-acetoxy-PhIP was monitored by HPLC; a major product representing >75% of the total eluate was observed and assigned as the N^2-acetoxy-PhIP product based on previously published results (*22, 23*). However, ≈15% of the remaining eluted material comigrated with PhIP or *N*-OH-PhIP standards, leaving <10% unidentified contaminant. Increased reaction times did not appear to increase the yield. The reaction mixture was immediately incubated with calf thymus DNA (see below).

In Vitro Formation of Macromolecular PhIP Adduct. High molecular weight calf thymus DNA was repurified by phenol extraction followed by dialysis against 20 mM 3-(*N*-morpholino)propanesulfonic acid (MOPS) buffer (pH 6.5) supplemented with 100 mM NaCl and 1 mM Na_2EDTA. The *N*-acetoxy-PhIP from the above reaction was added dropwise over 5 min to calf thymus DNA at 37 °C; then the reaction continued for 30 min longer. The DNA solution turned reddish-orange as the *N*-acetoxy-PhIP solution was added, due to formation of the azo-PhIP dimer byproduct of *N*-acetoxy-PhIP degradation (*23*). The reaction tube was purged with anhydrous nitrogen gas, and the reaction was done in the dark to prevent degradation of PhIP adduct. The adduction reaction was done with ratios of DNA base pairs to *N*-acetoxy-PhIP of 90, 60, or 30. The DNA was usually 1–2 mg/mL in MOPS buffer. Thus the relative volume of *N*-acetoxy-PhIP reaction solution added to the DNA was varied as well: from 1% v/v to 8% v/v, depending upon the ratio of ligand to base pairs, the concentration of the initial *N*-acetoxy-PhIP stock, and the DNA concentration. Since the *N*-acetoxy-PhIP solution contains much acetic anhydride, it is possible that acetylation of DNA bases occurred during the reaction. Performing the reaction with varying concentrations of acetic anhydride was used to help evaluate the effect of increased acetic anhydride concentration on PhIP adduct formation (see Discussion).

Table 1. PhIP Chromophore Absorption Characteristics

compound	absorbance max (nm)	extinction coeff. ($M^{-1}cm^{-1}$)	FWHM (cm^{-1})
PhIP[a]	314.5	17 700	3700
N-OH-PhIP	317	17 700	4200
N-O-Ac-PhIP	326	18 300	3900
dG-C8-PhIP	362		4500
DNA-PhIP adduct	355	≈20 000[b]	5000

[a] All PhIP metabolites and adducts in 20 mM phosphate buffer (pH 7.0) with 100 mM NaCl and 1 mM EDTA. [b] Manuscript in preparation.

After cessation of the reaction, PhIP chromophore that was not covalently bound to DNA was removed by five extractions with 1 volume of water-saturated 1-butanol followed by an ethanol precipitation of the DNA. The DNA pellet was resuspended in water and then extensively dialyzed against phosphate buffer (20 mM dibasic phosphate (pH 7.0) with 100 mM NaCl and 1.0 mM Na_2EDTA), or against 10 mM sodium cacodylate buffer (pH 7.0). The latter adduct solution was used for fluorescence quenching experiments with silver ion. PhIP chromophore noncovalently bound to DNA or free in solution was not usually detectable after the butanol extractions and dialysis, although some fluorescence signal from unadducted PhIP was occasionally observed in the adduct samples due to its high quantum yield. However, fluorescence experiments on adduct samples over several days liberated fluorophore with fluorescence characteristics very similar to that of *N*-OH-PhIP. Thus PhIP adduct appeared to be moderately labile, and accordingly PhIP adduct solutions were stored in the dark at temperatures <−35 °C.

Kinetics Measurement of the Decay of *N*-Acetoxy-PhIP. After activation, *N*-acetoxy-PhIP was diluted to 30 μM in MOPS buffer (20 mM MOPS (pH 6.5), 100 mM NaCl, and 1 mM Na_2-EDTA). The decay of *N*-acetoxy-PhIP was monitored by a Shimadzu UV-2101PC UV/vis spectrophotometer (Columbia, MD), with the sample maintained at 25 °C in 1 cm path length quartz cuvettes (4 mL volume). *N*-Acetoxy-PhIP in aqueous solution was determined to have a absorbance maximum at 323 nm (Table 1), but after 1 h degrades to two products with absorbance maxima at 317 and 360 nm (data not shown). Thus, the absorption of the *N*-acetoxy-PhIP solution was monitored at 325 nm in 1 min increments for at least 30 min. The decay of the acetylated PhIP was fitted to an exponential using the MathCAD software package from Math Soft, Inc. (Cambridge, MA).

^{32}P-Postlabeling of Adducted DNA. Small aliquots (<1 μg) of DNA modified by *N*-acetoxy-PhIP in vitro were used for the postlabeling analysis under nonintensification conditions according to previously reported methodologies (*27, 28*), except that the chromatography conditions were the following. Development in D1 was overnight in 2.3 M NaH_2PO_4 (pH 5.8), D2 was omitted, development in D3 was in 3 M lithium formate (pH 3.35) with 7 M urea, development in D4 was in 0.5 M Tris-HCl (pH 8.0) supplemented with 0.72 M LiCl and 7.25 M urea, and development in D5 was in 1.0 M NaH_2PO_4 (pH 6.0). Adduct levels were determined from Cerenkov counting of adducts excised from TLC plates (*27*).

Absorption Spectra of Macromolecular PhIP Adducts. PhIP-modified DNA samples (1–10 mM) were monitored using

a Shimadzu UV-2101PC spectrophotometer. Adducted DNA samples were maintained in 4 mL (1 cm optical path length) quartz cuvettes at 5 °C by thermoregulation of a Shimadzu water-jacketed cuvette holder. Spectra were typically obtained using the following ranges of parameters: 0.2−1.0 nm sampling interval, 0.5−2.0 nm bandpass, 200−700 nm/min scan speed. In practice, the higher-resolution settings afforded little or no resolution enhancement of already-broadened adduct spectra, so settings were chosen to minimize the time the sample was being probed by light.

Fluorescence Spectroscopy of Macromolecular PhIP Adducts. Adduct fluorescence was monitored using a Fluorolog-2 spectrofluorometer (F111A1 configuration) from Spex Industries (Edison, NJ). Spectra were obtained under the following conditions: 1.0 mm slitwidth (3.87 nm bandpass) for all excitation and emission monochromator slits, 0.5 nm sampling intervals, 0.2 s signal collection per sampling interval, and right angle fluorescence collection geometry used for solution fluorescence. In addition, all spectra were corrected to account for the variation of the Xe lamp excitation source. The concentrations of DNA base pairs and PhIP adduct chromophore in samples for fluorescence spectroscopy were typically 1 mM and ≤2 μM, respectively, corresponding to an adduct absorbency of ≤0.04 at λ_{max}. Solutions of PhIP-modified DNA were pipetted into 4 mL quartz cuvettes (1 cm optical path length) and were maintained at 5 °C during acquisition of spectra. Samples in the sample compartment were purged with anhydrous nitrogen gas for at least 20 min before spectra were acquired, and for the duration of the experiment, in order to prevent condensation from forming on the cuvette windows, and to remove dissolved oxygen from the adduct solutions. All spectra were analyzed using the software package accompanying the Fluorolog-2 instrument and plotted using Kaleidagraph (Synergy Software, Reading, PA).

For collection of excitation spectra, the fluorescence emission is collected at one wavelength, and the excitation source (λ_{ex}) is scanned over the region of fluorophore absorption. For a pure chromophore this usually generates, on an approximate level, the absorption spectrum of the fluorophore, using much less analyte than is required for absorption spectroscopy. For the macromolecular PhIP adduct samples, the emission monochromator was set at various wavelengths (λ_{em}) ranging from 355 to 465 nm, and for each setting of the emission monochromator, the excitation monochromator was scanned from 250 nm to λ_{em} −10 nm. Emission spectra are generated by exciting the fluorophore at a given wavelength (λ_{ex}) on the fluorophore's absorption spectrum, and then scanning the fluorescence emission. This technique gives the spectrum of the analyte fluorescence. For the PhIP adduct samples, the excitation source was set at various wavelengths ranging from 315 to 400 nm, and the fluorescence emission was scanned from λ_{ex} +10 to 500 nm. Fluorescence spectra of background samples (DNA + buffer + water) were always acquired in order to subtract out nonadduct contributions to the fluorescence signal, especially from the 3400 cm^{-1} Raman band due to the OH stretch of water.

The Effect of Fluorescence Quencher on PhIP Adduct Fluorescence Intensities. Fluorescence excitation and emission spectra were obtained after either Ag^+ or acrylamide was titrated to the adduct solutions. Silver ion in the form of $AgNO_3$ was titrated to PhIP adduct in 10 mM cacodylate buffer (pH 7.0) up to 0.2 mol of silver/mol of base. Acrylamide was titrated to PhIP adduct in a higher-salt buffer [20 mM dibasic phosphate (pH 7.0) supplemented with 100 mM NaCl and 1.0 mM Na_2-EDTA] up to 1.0 M. During titrations, fluorescence emission was monitored by exciting at 360 nm, and collecting the emission spectrum from 370 to 500 nm. Samples equilibrated >10 min before spectrum acquisition, and all spectra were acquired as the average of three scans. After the titrations were completed, many excitation and emission spectra were obtained in order to preferentially probe the different adduct species. For all adduct samples with quencher, fluorescence spectra of background samples consisting of buffer + DNA + silver were collected to obtain a pure fluorescence from adduct. Background fluorescence spectra were especially crucial for the silver-quenched samples, which tended to yield more background fluorescence.

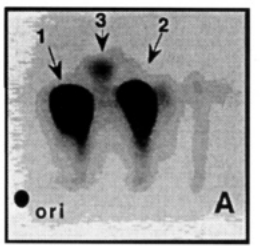

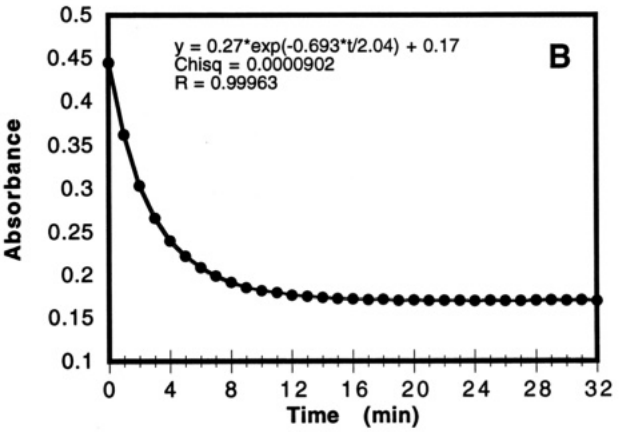

Figure 1. Panel A: ^{32}P-Postlabeling profile of 100 ng of calf thymus DNA modified in vitro by *N*-acetoxy-PhIP. The DNA was heavily modified and the postlabeling was performed under nonintensification conditions. The autoradiogram resulted from a 1 min exposure at −70 °C to Kodak XOMAT AR5 X-ray film. Panel B: The decay of *N*-acetoxy-PhIP in pH 6.5 MOPS buffer (20 mM) supplemented with 100 mM NaCl and 1 mM Na_2EDTA. The absorption was monitored at 325 nm (the λ_{max} of *N*-acetoxy-PhIP) with the cuvette maintained at 25 °C.

Results

Kinetics of DNA Adduction by *N*-Acetoxy-PhIP. Postlabeling profiles of calf thymus DNA modified by *N*-acetoxy-PhIP in vitro showed two major and several minor adduct spots after TLC separation (Figure 1A). The major adduct spot (spot 1) closest to the origin may consist of two adduct species which almost comigrate during the TLC separation, since spot 1 is always broader than spot 2, with two "tails" trailing down. Spot 1 is likely the 3′-phosphate of the dG-C8-PhIP adduct, which has previously been shown to migrate to this position during the TLC separation (*19, 22*). The relative adduct labeling (RAL) for this postlabeled PhIP-modified DNA yielded a value of approximately 0.0016 adduct/nucleotide, or 1 PhIP covalently bound per ≈600 bases.

The rate of DNA adduct formation by PhIP in pH 6.5 MOPS buffer should be similar to the rate of *N*-acetoxy-PhIP hydrolysis in the same buffer, since 2′-deoxyguanosine does not appear to catalyze the hydrolysis of *N*-acetoxy-PhIP: the kinetics was first order with respect to *N*-acetoxy-PhIP and zero order with respect to 2′-deoxyguanosine (*23*). Thus, *N*-acetoxy-PhIP (absorbance λ_{max} = 323 nm) in pH 6.5 MOPS buffer was allowed to decompose to solvolysis products (*23*), putatively either *N*-OH-PhIP (λ_{max} = 317 nm) or bis-azo-PhIP dimer (λ_{max} = 360 nm), with the reaction being monitored at 325 nm (Figure 1B). The *N*-acetoxy-PhIP proved to be unstable

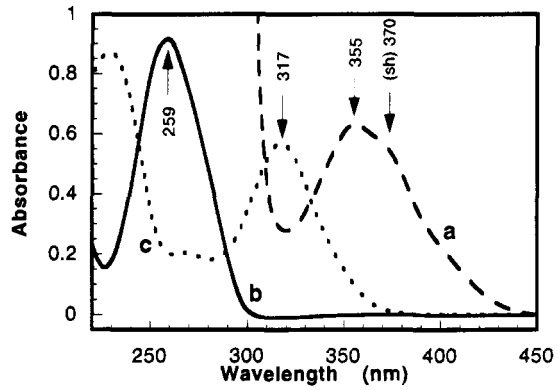

Figure 2. UV/vis spectrum of a high concentration (4.63 mg/mL or 7.3 mM bases) of calf thymus DNA modified in vitro by *N*-acetoxy-PhIP (spectrum a), plus the spectrum of its 100× dilution (spectrum b). Curve c shows the absorption spectrum of 33 μM *N*-OH-PhIP standard. All spectra described in Figure 2 were generated at ambient temperature with analyte in 20 mM phosphate buffer (pH 7.0) supplemented with 100 mM NaCl and 1 mM Na_2EDTA.

in pH 6.5 MOPS buffer. The decomposition of the carcinogen was fitted to a single exponential, yielding a half-life of 2.04 ± 0.02 min (Figure 1B), and thus was essentially completed by 10 min. However, since light from the UV/vis spectrophotometer was irradiating the sample continuously during the time course, it is possible that the rapidity of the *N*-acetoxy-PhIP decomposition was due partly to photolability.

UV/Vis Spectra of Macromolecular DNA-PhIP Adduct. Absorption spectra of PhIP, *N*-OH-PhIP, *N*-acetoxy-PhIP, and dG-C8-PhIP adduct standard were acquired in moderate ionic strength phosphate buffer. Absorption spectra of PhIP-modified macromolecular DNA in phosphate buffer were also generated after cessation of the *N*-acetoxy-PhIP reaction with DNA (Figure 2). The lowest-energy absorption bands of PhIP, *N*-OH-PhIP, and *N*-acetoxy-PhIP in aqueous buffers were nearly symmetrical and were characterized by maxima of 314.5, 317, and 323 nm (Figure 2 and Table 1). By contrast, the maxima of the lowest-energy absorbance bands of dG-C8-PhIP adduct standard and PhIP-adducted calf thymus DNA in aqueous buffer were 363 and 355 nm, respectively (Figure 2 and Table 1). Thus, the covalent modification of either guanine nucleoside or macromolecular DNA by PhIP resulted in an ultraviolet spectrum shifted to much lower energies (≈3500 cm^{-1}) compared to PhIP species not covalently bound to DNA (cf. spectra a and c). In addition, the highest-wavelength band of the macromolecular adduct (curve a) was blue-shifted 8 nm with respect to the dG-C8-PhIP standard, but possessed a prominent 370 nm shoulder, suggesting that more than one species of PhIP adduct was formed to highly polymerized DNA. Furthermore, the full width at half maximum (FWHM) of the DNA adduct 355 nm band was larger, at 5000 cm^{-1}, than was measured for other pure PhIP chromophore species (Table 1). In particular, the spectrum of dG-C8-PhIP adduct standard in aqueous solution yielded an FWHM of 4500 cm^{-1}.[2] These data taken together suggest heterogeneous DNA adduct formation by *N*-acetoxy-PhIP.

PhIP adduct was formed in high yield. Based upon HPLC separations of oligodeoxynucleotide–PhIP adduct (data not shown), the adduct extinction coefficient at 355

[2] In other organic solvents tested, the FWHM of dG-C8-PhIP was considerably lower, manuscript in preparation.

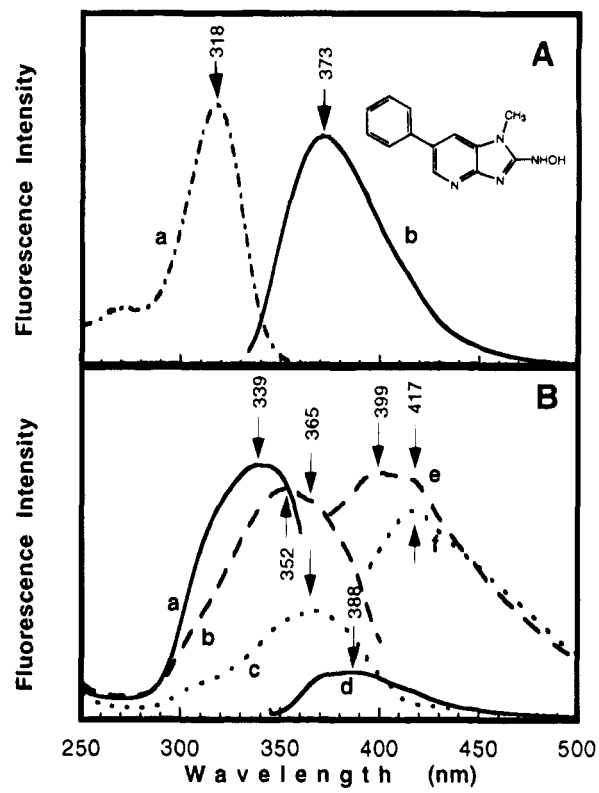

Figure 3. Panel A: Fluorescence excitation (a) and emission (b) spectra of 100 nM *N*-OH-PhIP in phosphate buffer [20 mM dibasic phosphate (pH 7.0) supplemented with 100 mM NaCl and 1 mM Na_2EDTA]. The emission and excitation monochromators were set to 380 and 320 nm for spectra a and b, respectively. Panel B: Fluorescence excitation (spectra a – c) and emission (spectra d – f) of PhIP-modified calf thymus DNA in phosphate buffer. The DNA concentrations were typically 1 mM bp, and the adduct binding density was ≈1 PhIP/500 bases DNA. The excitation spectra were acquired with the emission monochromators set at 375 (spectrum a), 417.5 (spectrum b), and 465 nm (spectrum c), and the emission spectra were acquired by exciting the adduct at 333 (spectrum d), 360 (spectrum e), and 380 nm (spectrum f). Excitation and emission monochromator slits were set at 1 mm (3.84 nm bandpass, panel A) or 2 mm (7.74 nm bandpass, panel B), and the spectra were all acquired at 5 °C. The wavelength reproducibility of spectra here was ±1 nm. The Raman scatter band due to the OH stretch mode of water has been subtracted from all spectra.

nm was estimated to be ≈20 000 M^{-1} cm^{-1}, similar to that of free PhIP at its lowest-energy λ_{max}. The DNA concentration was determined from the UV spectrum of a 100-fold dilution of the DNA adduct (spectrum b of Figure 2). The efficacy of *N*-acetoxy-PhIP covalent attachment to DNA was thus estimated to be ≈18%, typical for the in vitro protocol used in our study. For the particular sample depicted in Figure 2, approximately one DNA base in 400 was modified by a PhIP chromophore. This value of the binding efficiency of *N*-acetoxy-PhIP, while an estimation, is similar to the approximate value obtained by postlabeling (see Figure 1A).

Fluorescence Spectra of PhIP Metabolites. The fluorescence excitation and emission spectra of pure *N*-OH-PhIP in aqueous buffers were very broad and were characterized by excitation and emission maxima of 318 and 376 nm, respectively (Figure 3A). The fluorescence spectra of PhIP and *N*-acetoxy-PhIP had very similar profiles; fluorescence characteristics are given in Table 2. In aqueous buffers, *N*-acetoxy-PhIP is thought to decompose mainly to *N*-OH-PhIP (*23*). Upon binding of *N*-acetoxy-PhIP to DNA, we observed a highly fluorescent contaminant with spectral characteristics very similar

Table 2. PhIP Chromophore Fluorescence Characteristics

compound	exc max (nm)	em max (nm)	ΔE (cm^{-1})[a]	rel quantum yield[b]	FWHM (cm^{-1})	effect of silver[c]	effect of acrylamide	tentative conformation[d]
N-OH-PhIP[e]	317	374	4700	1.0	4100			
PhIP	315	369	4700	0.98	3400	45% quenched	quenched	groove-bound[f]
N-O-Ac-PhIP	317	377	5000	0.57	4500			
N-O-Ac-PhIP breakdown product	318	375	4600	unknown	4700	60% quenched	quenched	groove-bound
PA1	338–343	388–393	3800	<0.1	3600	quenched	unquenched	internal
PA2	368–370	396–398	1800	<0.1	2700	enhanced	unquenched	internal
PA3	348–352	397–402	3600	<0.1	3000	unquenched	slightly quenched	solvent-accessible
PA4	364–367	418–424	3700	≈0.01	3800	unquenched	quenched	solvent-accessible

[a] The Stokes shift, or separation in wavenumbers between the lowest-energy fluorescence excitation maximum and the fluorescence emission maximum. [b] These are relative to *N*-OH-PhIP standard and were measured by calculating the areas of fluorescence emission spectra in units of intensity times wavenumbers, given that the fluorophore concentrations were known. All spectrofluorometer parameters were identical for the compounds. [c] The silver was 300 μM and the DNA was 1.5 mM bases for the silver quenching studies. For the acrylamide quenching experiments, the acrylamide and DNA were 1.0 M and 1.5 mM bases, respectively. [d] Based on fluorescence quenching studies only. As discussed in the text, these assignments are very tentative if fluorescence lifetimes are unknown. [e] All spectra of compounds were generated with fluorophore in 20 mM phosphate buffer (pH 7.0) with 100 mM NaCl and 1.0 mM Na_2EDTA, with the exception of the fluorescence quenching studies of adduct performed with silver ion that were performed in 10 mM sodium cacodylate buffer (pH 7.0). [f] Reference 50.

to those of *N*-OH-PhIP standard (Figure 3A and Table 2). This contaminant did not appear to be adduct: it was easily removed by either butanol extractions or dialysis, and its absorbance and fluorescence spectra were greatly blue-shifted compared to adduct spectra, enabling an easy interpretation of adduct spectra even if some contaminant was present. We did not observe any noncovalently bound forms of *N*-OH-PhIP with spectra dissimilar to that of free compound, but the absorption and fluorescence spectra of noncovalently bound PhIP (*29*) do not undergo any significant change upon binding to DNA.

Fluorescence Spectra of Macromolecular DNA-PhIP Adducts. Fluorescence excitation and emission spectroscopies were performed on several PhIP-modified calf thymus DNA samples at 5 °C. Figure 3B depicts adduct excitation spectra with the emission monochromator positioned at three wavelengths (λ_{em}), and emission spectra holding the excitation wavelength at three wavelengths (λ_{ex}). As the excitation wavelengths were chosen to be lower in energy, the emission spectra of the adduct were accordingly red-shifted. At λ_{ex} = 333, 360, and 380 nm, the maxima of the fluorescence emissions were 388, 399, and 417 nm, respectively. The excitation spectra in Figure 3B were obtained by setting λ_{em} = 375, 417.5, and 465 nm and yielded excitation maxima at 339, 352, and 365 nm, respectively. (Note that only the lowest-energy fluorescence excitation bands were visible: DNA was present at high concentrations and absorbed most of the light <300 nm, at which wavelength the excitation spectra decreased to nearly zero intensity.) Some other values of λ_{ex} or λ_{em} yielded similar spectra (see Figure 4), but for the sake of brevity, here we only show some representative spectra of PhIP adducts. In general, the fluorescence excitation spectra of PhIP adduct without fluorescence quencher in solution suggested the presence of at least 3 adduct fluorophores with maxima of ≈340, ≈350, and ≈365 nm, and the fluorescence emission spectra suggested the presence of at least 3 adduct chromophores with maxima of ≈390, ≈400, and ≈417 nm. Thus, the covalent attachment of PhIP to highly polymerized DNA resulted in a substantial red-shifting of the adduct absorbance and fluorescence spectra with respect to free PhIP, *N*-OH-PhIP, or *N*-acetoxy-PhIP in solution. The magnitude of the red shift was 20–50 nm, depending on adduct species, and indicates a large disparity of $S_1 \leftarrow S_0$ energies among PhIP adducts, signaling a considerable adduct heterogeneity upon PhIP binding to DNA.

Characteristics of PhIP Adduct Fluorescence as the Excitation and Emission Wavelengths Are Varied. To further explore the nature of the PhIP-DNA adducts, we wish to extend the work from the last figure. In general, since luminescence originates from the $v = 0$ vibrational level of the S_1 state regardless of the extent the excitation energy exceeds this level, the luminescence maximum is essentially independent of the excitation wavelength (*30, 31*). If a fluorophore exists in a homogeneous environment during its excited-state lifetime, there will be no change in its fluorescence emission as the excitation energy is varied. Some small degree of shifting of fluorescence energies for a chemically pure fluorescent analyte may occur upon excitation at different wavelengths if that analyte is found in a heterogeneous environment, e.g., within a glassy matrix. Thus, fluorescent components in a mixture with sufficiently-resolved $S_1 \leftarrow S_0$ absorption bands should be resolvable as the mixture is excited at a wide range of wavelengths (*32, 33*).

One can evaluate the number of adduct fluorophores by measuring the fluorescence excitation maxima as the emission monochromator is incremented from 375 to 490 nm (Figure 4A). Because of the nature of luminescence (see above), adduct species with sufficiently separated $S_1 \leftarrow S_0$ absorption bands will appear as plateaus on this plot if their fluorescence emissions are also sufficiently separated in energy. As the wavelength of detection for adduct fluorescence emission (λ_{em}) was increased from 375 to 490 nm in 5 nm increments (Figure 4A), the presence of multiple fluorophores was manifested by a steady increase in the excitation maximum. There appeared to be two distinct phases in the plot of excitation maxima versus emission monochromator setting (Figure 4A). The first phase was represented by a gradually increasing shift in excitation maximum from 340 to 352 nm as λ_{em} was varied from 380 to 440 nm. Such a shift in excitation maxima probably indicates two or more adduct species with excitation maxima relatively close together, i.e., at ≈340 and ≈350 nm. The second phase was represented by a plateau in the excitation maximum at ≈365 nm as λ_{em} was set above 470 nm. Thus, the steady shift of the fluorescence excitation

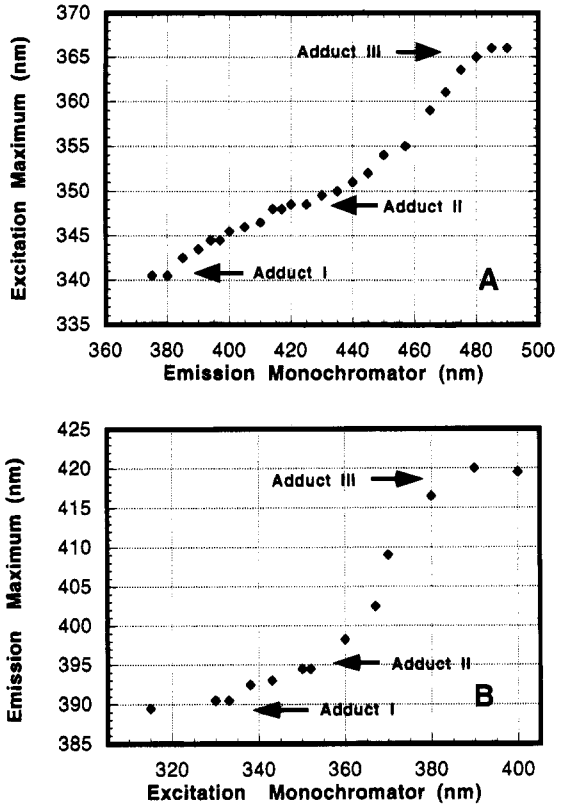

Figure 4. Panel A: Plots of fluorescence excitation maxima versus the emission monochromator setting (λ_{em}) for calf thymus DNA covalently modified by PhIP. Panel B: Plots of fluorescence emission maxima versus the excitation wavelength (λ_{ex}) for PhIP-modified calf thymus DNA. The DNA was typically 1 mM bp in 20 mM phosphate buffer (pH 7.0) supplemented with 100 mM NaCl and 1 mM Na_2EDTA. Discrete adduct species appear as plateaus in the plot. All fluorescence spectra were acquired as discussed in the Materials and Methods section and Figure 3. All spectra were acquired at 5 °C, and the wavelength reproducibility of spectra was ±2 nm.

maxima as λ_{em} was varied suggests a highly heterogeneous distribution of PhIP adducts.

Figure 4B shows plots of fluorescence emission maxima versus excitation wavelength for PhIP-adducted DNA in solution. Two distinct fluorescence emission plateaus were observed; one from 389 to 400 nm, and the other from 416 to 420 nm. The fluoresence emission rose gradually but steadily from 389 to 398 nm as the excitation wavelength was incremented from 315 to 360 nm, suggesting that more than one adduct fluoresces in the 389–398 nm range. Combining the results from panels A and B from Figure 4, PhIP adduct species with absorbance λ_{max} from 340 to 350 nm probably correspond to the PhIP adducts with fluorescence maxima from 389 to 398 nm. Furthermore, the fluorophore with fluorescence excitation and emission maxima of 365 and 420 nm, respectively, probably corresponds to the same adduct.

Because the spectra of PhIP adduct were broad and showed no vibronic structure, it was necessary to perform fluorescence quenching studies on the adduct to evaluate the number of adducts formed and the conformations these adducts might assume upon covalent DNA binding. Here we stress, in terms of establishing the conformation of adduct, that fluorescence quenching of adduct will be a function of chromophore fluorescence lifetime (*33–36*) as well as conformation of the DNA-bound fluorophore (i.e., the accessibility of the fluorophore to quencher).

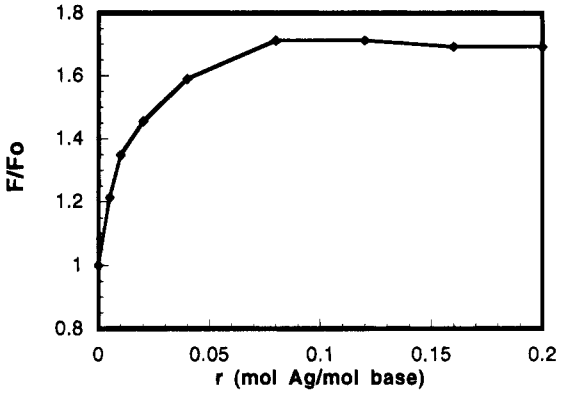

Figure 5. Titration with $AgNO_3$ of PhIP-modified calf thymus DNA (1.5 mM bases) in 10 mM cacodylic acid buffer (pH 7.0). F/F_0 is the spectrum intensity after each titration divided by the intensity of the fluorescence before quencher was added. The adduct was excited by 360 nm light, and the fluorescence emission monitored at 397 nm. The temperature was maintained at 10 °C, and all slits were set to 1.0 mm (3.87 nm bandpass).

Thus, reliance on quenching data alone to assign conformation may mislead, but an evaluation of PhIP adduct fluorescence kinetics is beyond the scope of this paper.

Fluorescence of PhIP Adducts in the Presence of Silver Quencher. A PhIP adduct sample formed by combining a 30× molar excess of DNA bp with *N*-acetoxy-PhIP was titrated with silver ion and excited with 360 nm light after each titration. The emission intensity was measured at 397 nm, the maximum of the overall fluorescence emission. The most obvious effect of titrating PhIP adduct with silver was to increase adduct fluorescence (Figure 5). In the presence of 0.2 mol of Ag/mol of DNA bases, the adduct fluorescence intensity was 1.7 times greater than if no silver was present (F/F_0 = 1.7). By contrast, the fluorescence from free PhIP in solution is strongly quenched by silver ion, with only 2% of initial fluorescence generated after titrating to 30 μM Ag^+ (*29*).

Figure 6A shows fluorescence excitation (λ_{em} = 400 nm) and fluorescence emission (λ_{ex} = 367 nm) spectra of the adduct with silver-enhanced fluorescence. Spectrum a shows the unquenched adduct, with an excitation maximum of 351 nm. But upon addition of silver ion, a band appeared at 370 nm (spectrum b). Spectrum c is b − a, and yielded what the silver enhanced. A strongly-fluorescent adduct fluorophore with an excitation maximum of 372 nm was apparent, but these spectra indicated that Ag^+ also quenched some or all of the *N*-OH-PhIP fluorescence (λ_{max} = 319 nm). It did not appear that the adduct with a fluorescence maximum of 351 nm was either quenched or enhanced. When the adduct was excited at 367, the initial fluorescence emission at 399 nm (spectrum d) was greatly enhanced upon addition of silver (spectrum e). Subtracting e − d shows that the adduct fluorescence which was enhanced has an emission maximum at 397 nm (spectrum f). Based on the fluorescence emission energy, this silver-enhanced adduct with excitation and emission maxima of 370 and 397 nm, respectively, is denoted PA2 (Table 2).[3] The enhancement of fluorescence upon DNA binding by silver ion has been attributed to an induced change in DNA conformation

[3] The four observed adducts were assigned the nomenclature PA*i*, where "PA" denotes PhIP Adduct and i = 1–4 gives the order of fluorescence emission band energies, with 1 the highest and 4 the lowest energy, respectively.

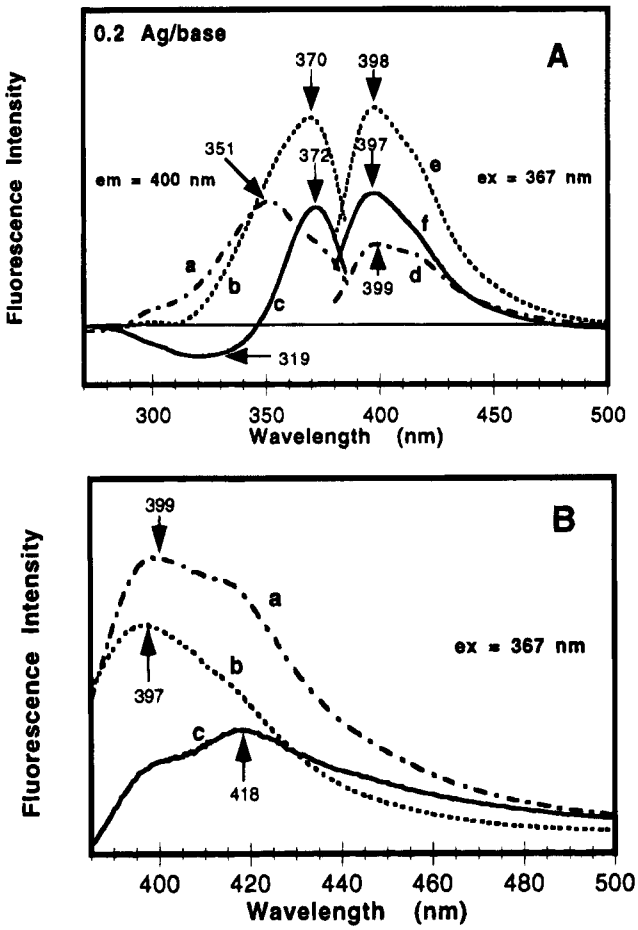

Figure 6. Panel A: Fluorescence excitation and emission spectra showing the silver-induced enhancement of a PhIP adduct. The DNA base concentration is 1.5 mM, with the silver present at a ratio of 0.2 mol of Ag^+/mol of DNA bases. Excitation (λ_{em} = 400 nm) and emission (λ_{ex} = 367 nm) spectra a and d, respectively: Adduct sample without quencher. Excitation and emission spectra b and e: Adduct sample + silver. Excitation and emission spectra c and f: Difference spectra of (adduct + silver) − (adduct − silver), showing what silver actually enhanced. Note that the excitation spectrum c has a negative peak at 319 nm because some *N*-OH-PhIP contaminant in the sample is quenched by silver. Here and below for all silver quenching experiments, T = 5 °C, and all slits = 3.87 nm bandpass. The adduct is in low-salt 10 mM cacodylate buffer (pH 7.0). Panel B: Fluorescence emission spectra (λ_{ex} = 367 nm) showing the effect of silver ion on the low-energy fluorescence of PhIP-modified DNA. Spectrum a shows adduct fluorescence in the absence of silver, spectrum b shows the adduct fluorescence enhanced by silver, and spectrum c is a − b, and shows what acrylamide did not enhance. Note that spectra a and b correspond to spectra a (times 2.3) and c, respectively, of panel A.

(*37*), with a concommitant change in adduct configuration from helix-internal to external (*35, 38*). For some adducts this results in increased fluorescence quantum yields, and in such cases suggests an adduct moiety that is sequestered from solvent before the addition of silver.

Interestingly, the emission maximum of the adduct sample without silver is 399 nm (spectrum d), suggesting an adduct species with fluorescence unquenched or unenhanced by silver and which exhibits an emission maximum of ≈400 nm. This adduct probably corresponds to the species that exhibits an excitation band of 351 nm and is denoted PA3 in Table 2 (cf. excitation and emission spectra a and d, respectively, of Figure 6A).

It can be seen in Figure 6A that the fluorescence from the adduct in the absence of silver (spectrum d) has a much more pronounced shoulder at ≈420 nm than that from the adduct + silver (spectrum e, Figure 6A). This indicates that an adduct with a fluorescence emission maximum of ≈420 nm was not enhanced when silver was added to solution. To further verify this, a spectrum of the adduct component whose fluorescence was enhanced by silver (spectrum b, Figure 6B) was subtracted from unquenched adduct spectra (spectrum a, Figure 6B) in order to generate the spectrum of adduct unaffected by silver quencher (spectrum c, Figure 6B). The result is spectrum c in Figure 6B, showing that an adduct with a fluorescence maximum of 418 nm was not noticeably enhanced by the addition of silver.

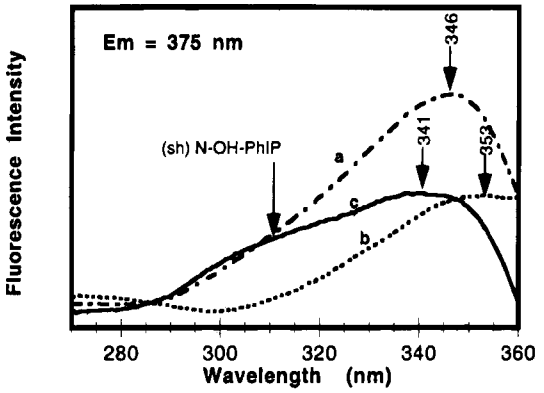

Figure 7. Fluorescence excitation spectra (λ_{em} = 375 nm) from PhIP adduct in the presence or absence of silver quencher. The DNA was 1.5 mM bases in 10 mM cacodylate buffer (pH 7.0). Spectrum a shows the fluorescence from adduct in the absence of silver ion, and spectrum b shows adduct fluorescence after silver was added. Spectrum c is spectrum a − spectrum b and shows what particular PhIP adduct silver actually quenched.

Holding the emission monochromator at 375 nm, we observed two distinct adducts with very different quenching characteristics when silver was added (Figure 7). Upon addition of silver ion, a fluorescence excitation band at 353 nm was observed; this adduct was probably the same adduct PA3 observed in Figure 6A (see also Table 2). The fluorescence from the adduct appeared to be unaffected by silver and thus was suggestive of a solvent-accessible adduct. But a higher energy adduct fluorescence characterized by a 341 nm excitation band was strongly quenched, along with a minor *N*-OH-PhIP fluorescence component (spectrum c, Figure 7). The adduct with the characteristic 340 nm excitation band appeared to correspond to an adduct with a fluorescence emission maximum of ≈390 nm and was denoted PA1 (see Table 2; emission spectra not shown).

The Fluorescence of PhIP Adducts in the Presence of Acrylamide Quencher. Figure 8, spectra a and d, shows the fluorescence excitation and emission spectra, respectively, of PhIP-DNA adduct in the absence of acrylamide quencher. Spectra b and e show adduct fluorescence in the presence of acrylamide, and spectra c and f show the adduct fluorescence component quenched by acrylamide. The addition of 1.0 M acrylamide to PhIP adduct solutions did not efficiently quench the fluorescence emission (λ_{max} = 398 nm) from adduct PA3 absorbing with λ_{max} = 350 nm (spectra e and b, respectively). However, acrylamide did efficiently quench the fluorescence emission (λ_{max} = 421 nm) from an adduct species absorbing with λ_{max} = 364 nm (spectra f and c, respectively). This adduct appears identical to the one with fluorescence yield unaffected by silver (see Figure 6B) and was assigned as PA4. The effect of silver and

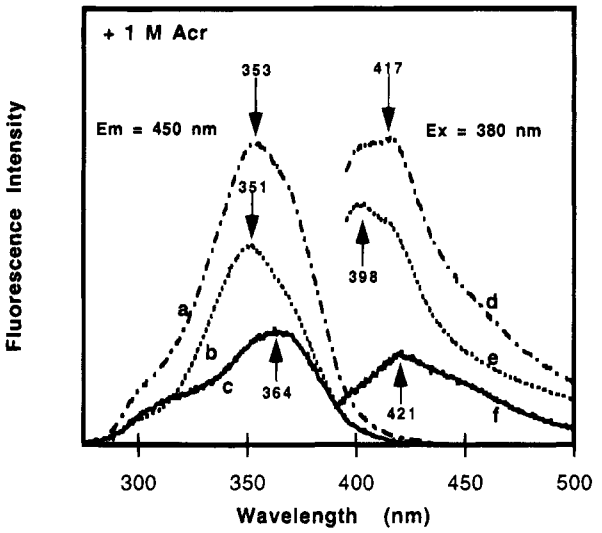

Figure 8. Fluorescence excitation (λ_{em} = 450 nm) and emission (λ_{ex} = 380 nm) spectra of macromolecular DNA-PhIP adduct in the presence or absence of 1.0 M acrylamide quencher. Here and for all acrylamide quenching experiments, T = 5 °C, all slits were set at 3.87 nm bandwidth, and samples were in 20 mM phosphate buffer (pH 7.0) supplemented with 100 mM NaCl and 1.0 mM Na_2EDTA. The DNA was 1.5 mM in bases. The top spectra (a and d) depict the fluorescence of adduct in the absence of quencher, the middle spectra (b and e) show the fluorescence of adduct in the presence of 1.0 M acrylamide quencher, and the bottom spectra (c and f) show the fluorescence that was quenched by acrylamide.

acrylamide quencher on PA4 suggests that this PhIP adduct is groove-bound or solvent-accessible.

Figure 7 showed that silver effectively quenched the adduct fluorescence with λ_{max} = 340 nm (PA1), but not the fluorescence from PA3 (λ_{max} = 350). In Figure 9A we examined the fluorescence of PA1 and PA3 in the presence of acrylamide by exciting at 367 nm (see Figure 9A emission spectra), and we also generated excitation spectra by detecting fluorescence at 400 nm. Under these conditions of lower-wavelength λ_{ex} and λ_{em}, we should preferentially detect PA1 and PA3 over PA4. Upon the addition of acrylamide, we observed some quenching of adduct fluorescence. The bottom curves of Figure 9A show the excitation (left) and emission spectra (right) of what acrylamide actually quenched. We observed a fluorescence emission with λ_{max} = 421 nm, but with less relative intensity since, relatively speaking, more adduct PA1 and PA3 was excited. We also observed a fluorescence emission shoulder (spectrum f) at ≈400 nm, and an adduct excitation band that was a prominent shoulder on the quenched fluorescence from *N*-OH-PhIP (spectrum c). Subtracting the fluorescence from authentic *N*-OH-PhIP standard from the spectrum of quenched adduct fluorescence yielded the spectrum of quenched adduct fluorescence alone without *N*-OH-PhIP contribution (Figure 9B). The λ_{max} of this adduct was ≈348 nm, suggesting that it was PA3 fluorescence which was quenched more than PA1 fluorescence. Nonetheless, even the fluorescence from PA3 clearly was not efficiently quenched. We therefore assigned PA1 as being internal, since its fluorescence was quenched efficiently by silver and not by acrylamide. We tentatively assigned PA3 as being partially solvent-accessible, since it was weakly quenched by acrylamide but unquenched by silver (Figures 7 and 9). This weakly quenched excitation band from PA3 appeared to correspond to a modestly quenched fluorescence emission with λ_{max} = 399 nm (Figure 9A emission spectra, and other data not shown).

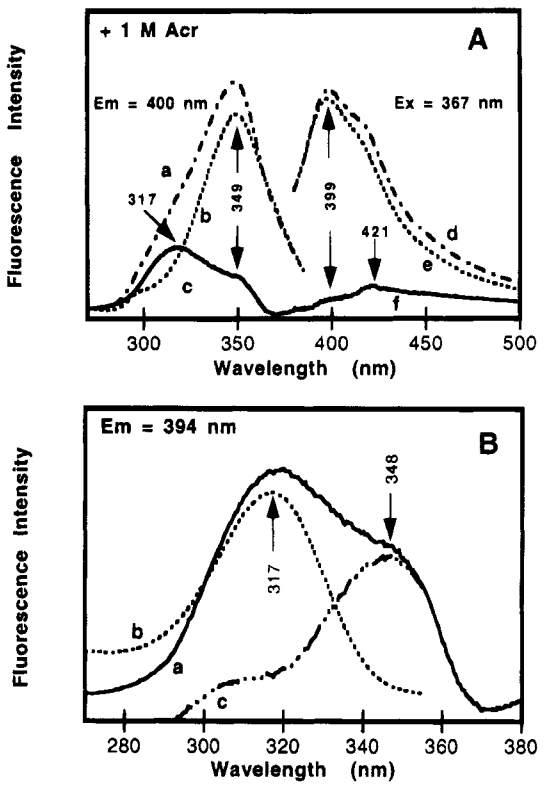

Figure 9. Panel A: Fluorescence excitation spectra a, b, c (λ_{em} = 400 nm) and emission spectra d, e, f (λ_{ex} = 367 nm) of PhIP adduct with and without acrylamide quencher. The DNA was 1.5 mM in bases; and T = 5 °C. Spectra a and d represent the fluoresence of adduct in the absence of acrylamide, spectra b and e represent the fluorescence of adduct in the presence of quencher, and spectra c and f (spectra a and d − spectra b and e, respectively) show what was actually quenched by acrylamide. Panel B: Fluorescence excitation spectra (λ_{em} = 394 nm) of PhIP adduct showing the identity of the higher-energy adduct quenched by acrylamide, and the extent of the quenching. Spectrum a shows the adduct fluorescence excitation quenched by acrylamide (unquenched − quenched adduct fluorescence). Spectrum b is the fluorescence excitation of *N*-OH-PhIP standard, and spectrum c is spectrum a −spectrum b and depicts the quenched higher-energy adduct fluorescence only without interfering *N*-OH-PhIP fluorescence signal.

A summary of fluorescence characteristics of all adducts is given in Table 2. There are some interesting spectral distinctions between unadducted PhIP chromophore and PhIP chromophore covalently bound to DNA. First, the lowest-energy absorption bands of PhIP adduct are considerably red-shifted with respect to the lowest-energy absorption bands of unadducted PhIP species (Table 1). Given this phenomenon, the fluorescence excitation and emission bands of PhIP adduct were correspondingly shifted to much lower in energy, as expected, with the highest-energy adduct emission maximum (388 nm) red-shifted 11 nm with respect to *N*-acetoxy-PhIP (377 nm, see Table 2). These data are in striking contrast with the spectral characteristics of benzo[*a*]pyrene diol epoxide (BPDE)−DNA adducts, in which the absorption and fluorescence emission bands of the groove-bound adduct and the quasi-intercalated BPDE adduct were only red-shifted 2 and 8 nm, respectively, with respect to free BPDE (*36*).

The FWHMs were calculated from the various spectra shown in this paper, but only where the fluorescence from a reasonably "pure" species is given (Table 2). In reality, this occurred as a byproduct of strong quenching by either silver or acrylamide, eliminating the fluorescence of at least one adduct species. There did not appear to be a

correlation between adduct spectral bandwidth and conformation. But all adduct bandwidths appeared to be less than those of either *N*-OH-PhIP or *N*-acetoxy-PhIP. We also calculated the Stokes shifts (ΔE), or the energies between the adduct excitation and emission maxima, and some striking trends were apparent. If adducts form exciplexes with considerable charge-transfer character, then larger ΔE values often correspond to more polar fluorophore environments (*39*). ΔEs were much larger for free and noncovalently bound PhIP species (4600–5000 cm^{-1}) than for adducts (1800–3600 cm^{-1}). In addition, the adduct exhibiting strongly enhanced fluorescence upon addition of silver ion (PA2) had a very small energy gap between fluorescence excitation and emission bands compared to that of the other adducts: 1800 cm^{-1} compared to 3400–3800 cm^{-1}. The much smaller ΔE for adduct PA2 is consistent with the quenching experiments, which indicate a helix-internal conformation of PA2 before the addition of silver. Thus, the lower polarity of the environment surrounding this adduct confirms the silver quenching data and suggests that PA2 may be in close contact with the aromatic bases of DNA.

Discussion

The reaction of *N*-acetoxy-PhIP with calf thymus DNA efficiently formed DNA-bound chromophores that could not be dialyzed or phase-partitioned from the DNA solution, indicating strongly that these chromophores were DNA adducts. All data presented herein strongly suggest that activated *N*-acetoxy-PhIP forms a highly heterogeneous distribution of DNA adducts. Adduct fluorescence excitation spectra shift significantly to lower energy as the emission monochromator is set to collect lower-energy adduct fluorescence. Thus, the adduct fluorescence excitation spectra were not similar in appearance to the absorption spectra, a very reliable sign of fluorophore heterogeneity (*34*). In addition, it appeared that, of the sum total of adduct fluorescence, some fluorescence was quenched by silver and some by acrylamide. In fact, there appeared to be at least four PhIP adducts, denoted PA1–PA4, distinguishable by fluorescence spectroscopy (Table 2). Two adducts, PA1 and PA2, did not appear to be accessible to solvent. Adduct PA3 appeared partially accessible to solvent, and PA4 appeared to be quite accessible to surrounding solvent. Our data also show that adducts were easily distinguishable from unreacted *N*-OH-PhIP, which may be a prominent breakdown product from *N*-acetoxy-PhIP (*23*). Adduct absorption, fluorescence emission, and fluorescence excitation spectra were all considerably red-shifted with respect to spectra generated from *N*-OH-PhIP contaminant in solution. In addition, adduct fluorescence excitation and emission bands were separated by a much smaller difference in energy than was observed for noncovalently bound PhIP species in solution.

Although fluorescence quenching clearly showed the formation of a heterogeneous distribution of PhIP-DNA adducts in vitro, it is a more ambiguous indicator of conformation. The quenching of fluorescence from one fluorophore is given by the Stern–Volmer equation:

$$F_0/F = 1 + \tau_0 K[Q] \quad (1)$$

where F_0 and F are the fluorescence intensities in the absence and presence of quencher with concentration [Q], respectively; τ_0 is the fluorescence lifetime when quencher is absent; and K is the bimolecular encounter rate (*34–36*). It can be seen that fluorescence quenching is proportional to the fluorescence decay time τ_0 and the molecular accessibility K. If the fluorescence lifetime is very short, then very little fluorescence quenching will occur even if the fluorophore is highly accessible to quencher. But if more than one fluorophore is present, as was apparent here, then the Stern–Volmer relation can be given as defined by Geacintov *et al.* (*40*):

$$F_0/F = \sum(f_i(\lambda)/(1 + \tau_i K_i[Q])^{-1}) \quad (2)$$

The meanings of all symbols are the same as above, except that $f_i(\lambda)$ denotes the fraction of total fluorescence contributed to the whole by each component i when excitation occurs at wavelength λ. Thus for multiple fluorophores in solution the efficiency of quenching is a function of the heterogeneity of the sample as well as a function of τ_i and K_i.

The fluorescence quenching data do not generate high-resolution results. An assignment of "external" or solvent-accessible often suggests a groove-bound moiety (*38, 40–42*). Conversely, an adduct identified as "interior" or inaccessible to solvent may be pseudo-intercalated (*40, 43*), in which the adduct stacks with the nearest-neighboring DNA bases. It is possible to envision other conformations, however, in which the adduct severely disrupts the helix structure, making it difficult to evaluate the PhIP configuration from quenching data. Further, there are intermediate conformations that are partially solvent-accessible: low-temperature fluorescence studies of BPDE adducts reveal a subset of adducts in which the pyrenyl moiety exhibits some base-stacking interaction with the DNA and is partly quenched by acrylamide (*44–46*). The PhIP adduct characterized by an excitation maximum of 348–352 nm and an emission maximum of 398–402 nm (PA3) may represent this type of adduct; its fluorescence is unquenched by silver and slightly quenched by acrylamide.

The fluorescence characteristics of PA4 (Table 2) are very similar to those of authentic dG-C8-PhIP standard, which has an absorbance maximum of 362 nm (Table 1) and a fluorescence emission maximum of 418 nm (data not shown). Hence adduct PA4, with excitation and emission maxima of 365 and 420 nm, respectively, was very likely formed by *N*-acetoxy-PhIP adduction through the C8 position of guanines. Adduct PA4 has also been tentatively identified as a groove-bound or solvent-exposed adduct by fluorescence quenching experiments. Again, we stress that quenching studies do not give unequivocal results if the fluorescence kinetics are not known. But in this context it is interesting to note the results of recent energy minimization modeling of PhIP covalently bound to a duplex heptanucleotide through the C8 position of the central guanine (*26*). The lowest energy structure was similar to that published previously for the dG-C8-aminofluorene adduct (*47*) and is characterized by the modified guanine in the *syn* orientation with the carcinogen moiety in the minor groove pointing in the 3′ direction of the modified strand.

The question remains as to whether any of the adducts result from covalent addition to nucleophilic centers of guanine bases other than the C8 position. The evidence presented here is quite inconclusive. The postlabeling data for PhIP modified DNA usually shows two, and often three, major PhIP adduct spots. The postlabeled 3′-phospho-dG-C8-PhIP adduct standard comigrates with

the PhIP-DNA adduct spot closest to the origin, usually denoted spot 1 (*22*). The other postlabeled adducts appear to be more polar, but these need not result from adduction to a different position on the guanine. Polar PhIP adducts could be breakdown or oxidation products of the dG-C8-PhIP adduct formed spontaneously after adduction to the DNA, in a manner similar to the aflatoxin B_1 formamidopyrimidine adduct (*48*), or might be artifacts of the enzymatic hydrolysis (*49*) and TLC separation needed for the postlabeling assay. Furthermore, the postlabeling assay can separate isomers of an adduct. For example, isomers of *anti*-BPDE covalently bound to guanines can be resolved on TLC plates after being postlabeled (*50*). But one spot resulting from the postlabeling assay can also represent multiple adduct species since adducts of different chemical identity can comigrate on TLC plates, such as some benzo[*c*]phenanthrene–adenosine adduct stereoisomers (*51*). Thus, the three spots revealed by the postlabeling of PhIP-modified DNA could also represent more than three chemically-distinct adducts.

In this study, the various adducts were observed to have quite different absorption and fluorescence characteristics. The lowest-energy absorbance maximum of macromolecular PhIP adduct generated in vitro was 355 nm (Figure 2), but the adduct fluorescence excitation band energies ranged from 340 to 370 nm, and the corresponding emission band wavelengths ranged from 390 to 420 nm. It is possible that adducts formed by covalent attachment to a different reactive group might have very different absorption and fluorescence characteristics. We know that for two other aromatic amine carcinogens, MeIQx and IQ, an adduct can also be formed to the exocyclic amine group of guanine bases through a bond directly to an aromatic ring carbon of the heterocyclic amine (*24, 25*). In these cases, the absorption spectra were quite different than if the adduct was to the C8 position of guanines. But there are alternative explanations: there is a strong possibility that adduct formed at the C8 position of guanines (probably PA4) spontaneously decomposes to PA1, PA2, or PA3 adducts having higher-energy fluorescence emissions. If so, these might occur in vivo and be critical in PhIP-induced carcinogenesis. Also, for some conformers of the dG-C8-PhIP adduct, there could be intramolecular hydrogen bonds or proton-transfer interactions that could effectively shift the absorption and fluorescence spectra to higher energies.

From the absorption spectra, adduct PA4 appeared to comprise a significant fraction of the total adduct. The absorbance maximum was 355 nm, with a pronounced shoulder at 370 nm (Figure 2). If very little PA4 were present, the maximum would likely be <350 nm, with no shoulder at 370 observed. However, the fluorescence analysis only showed "pure" PA4 emission spectra when λ_{ex} exceeded 390 nm and "pure" excitation spectra when λ_{em} exceeded 480 nm. But adduct PA1, PA2, and PA3 generated much more intense fluorescence spectra at a wide range of wavelengths. Thus, adduct PA4 does not appear to have as high a quantum yield as adducts PA1, PA2, and PA3. Although we can only give a qualitative estimate of the amount of PhIP chomophore bound to the DNA (see Figures 1 and 2), we nonetheless can assign an approximate PA4 quantum yield that is ≈1% that of free PhIP. The relative quantum yields of PA1, PA2, and PA3 may be as high as 10-fold higher, but still less than those for noncovalently bound PhIP, *N*-OH-PhIP, or *N*-acetoxy-PhIP (Table 2). The degree of fluorescence quenching of PA4 compared to nonadducted PhIP is extensive and comparable in magnitude to that experienced by BPDE upon binding to guanine residues (*40, 52*). For example, BPDE fluorescence is quenched if covalently bound to guanine bases, but not if to adenine bases (*53–55*). However, PhIP has not yet been proven to bind to adenines, and at any rate adenosines could facilitate strong PhIP adduct quenching if the relative redox potentials of the adenosine and PhIP moieties lead to efficient electron-transfer reactions (*39, 56*).

One final issue to address is the identity of adduct PA2, which is characterized by an energy gap of 1800 cm^{-1} between the fluorescence excitation (λ_{max} = 370 nm) and emission (λ_{max} = 397 nm) bands, far less than that observed for other adducts. One explanation for this much smaller Stokes shift is that PA2 is quasi-intercalated and in a nonpolar environment. Another explanation is that PA2 possesses an acetyl group. In our reaction protocol, the acetic anhydride is added with the activated *N*-acetoxy-PhIP to the DNA when the in vitro adduction occurs. We observed larger quantities of PA2 formed if the concentration of acetic acid and acetic anhydride was higher in the adduction reaction (data not shown). Interestingly, it also appeared that more PA4 was formed if the concentration of *N*-acetoxy-PhIP in the DNA solution was decreased. To further evaluate the effect of acetic acid and acetic anhydride on PhIP adduct formation to macromolecular DNA, we are presently binding *N*-OH-PhIP directly to DNA in pH 5.0 citrate buffer (*22*), without any activation to *N*-acetoxy-PhIP prior to adduction.

In summary, *N*-acetoxy-PhIP appeared to form a highly heterogeneous mixture of adducts to macromolecular DNA in vitro. Of great import is whether these adducts are also formed in vivo upon exposure to PhIP. The evidence thus far tentatively supports the hypothesis that a heterogeneous distribution of adducts is also formed in vivo. The postlabeling profiles of the PhIP-modified DNA used in this study were very similar to the profiles of DNA extracted from the tissues of rodents dosed with PhIP (manuscript in preparation). The adduct structures responsible for spots 2 and 3 of the PhIP adduct postlabeling profiles are unknown, but are presently being elucidated in our laboratory.

Acknowledgment. We wish to thank Professor Nick Geacintov for helpful discussions pertaining to this work. This work was performed under the auspices of the U.S. Department of Energy by the Lawrence Livermore National Laboratory under Contract W-7405-ENG-48 and partially supported by NIH Grant CA55861 and the U.S. Army Medical Research Development Command (Contract MM4559FLB).

References

(1) Felton, J. S., and Knize, M. G. (1990) Heterocyclic amine mutagens/carcinogens in foods. In *Handbook of experimental Pharmacology* (Cooper, C. S., and Grover, P. L., Eds.) Vol. 94/I, pp 471–502, Springer-Verlag, Berlin and Heidelberg.

(2) Knize, M. G., Cunningham, P. L., Griffin, E. A., Jr., Jones, A. L., and Felton, J. S. (1994) Characterization of mutagenic activity in cooked grain food products. *Food Chem. Toxicol.* **32**, 15–21.

(3) Manabe, S., Suzuki, H., Wada, O., and Ueki, A. (1993) Detection of the carcinogen 2-amino-1-methyl-6-phenylimidazo[4,5-*b*]pyridine in beer and wine. *Carcinogenesis* **14**, 899–901.

(4) Jagerstad, M., Laser-Reutersward, A., Oste, R., and Hayatsu, T. (1983) Creatinine and Malliard reaction products as precursors

of mutagenic compounds formed in fried beef. In *The Malliard Reaction in Foods and Nutrition* (Waller, G. R., and Feather, M. S., Eds.) ACS Symposium Series No. 215, pp 507–519, American Chemical Society, Washington, DC.

(5) Felton, J. S., Knize, M. G., Shen, N. H., Andresen, B. D., Bjeldanes, L. F., and Hatch, F. T. (1986) Identification of the mutagens in cooked beef. *Environ. Health Perspect.* **67**, 17–24.

(6) Felton, J. S., and Knize, M. G. (1991) Occurrence, identification, and bacterial mutagenicity of heterocyclic amines in cooked food. *Mutat. Res.* **259**, 205–217.

(7) Matsumoto, T., Yoshida, D., and Tomita, H. (1981) Determination of mutagens, amino-alpha-carbolines in grilled foods and cigarette smoke condensate. *Cancer Lett.* **12**, 105–110.

(8) Felton, J. S., Knize, M. G., Shen, N. H., Lewis, P. R., Andresen, B. D., Happe, J., and Hatch, F. T. (1986) The isolation and identification of a new mutagen from fried beef: 2-amino-1-methyl-6-phenylimidazo[4,5-*b*]pyridine (PhIP). *Carcinogenesis* **7**, 1081–1086.

(9) Knize, M. G., and Felton, J. S. (1986) The synthesis of the cooked-beef mutagen 2-amino-1-methyl-6-phenylimidazo[4,5-*b*]pyridine and its 3-methyl isomer. *Heterocycles* **24**, 1815–1819.

(10) Ito, N., Hasegawa, R., Sano, M., Tamano, S., Esumi, H., Takayama, S., and Sugimura, T. (1991) A new colon and mammary carcinogen in cooked food, 2-amino-1-methyl-6-phenylimidazo[4,5-*b*]pyridine (PhIP). *Carcinogenesis* **12**, 1503–1506.

(11) Wakabayashi, K., Nagao, M., Esumi, H., and Sugimura, T. (1992) Food-derived mutagens and carcinogens. *Cancer Res.* **52**, 2092s-2098s.

(12) Esumi, H., Ohgaki, H., Kohzen, E., Takayama, S., and Sugimura, T. (1989) Induction of lymphoma in CDF1 mice by the food mutagen, 2-amino-1-methyl-6-phenylimidazo[4,5-*b*]pyridine. *Jpn. J. Cancer Res.* **80**, 1176–1178.

(13) Kaderlik, K. R., Minchin, R. F., Mulder, G. J., Ilett, K. F., Daugaard-Jensen, M., Teitel, C. H., and Kadlubar, F. F. (1994) Metabolic activation pathway for the formation of DNA adducts of the carcinogen 2-amino-1-methyl-6-phenylimidazo[4,5-*b*]pyridine (PhIP) in rat extrahepatic tissues. *Carcinogenesis* **15**, 1703–1709.

(14) Holme, J. A., Wallin, H., Brunborg, G., Soderlund, E. J., Hongslo, J. K., and Alexander, J. (1989) Genotoxicity of the food mutagen 2-amino-1-methyl-6-phenylimidazo[4,5-*b*]pyridine (PhIP): formation of 2-hydroxamino-PhIP, a direct-acting genotoxic metabolite. *Carcinogenesis* **10**, 1389–1396.

(15) Frandsen, H., Rasmussen, E. S., Nielsen, P. A., Farmer, P., Dragsted, L., and Larsen, J. C. (1991) Metabolic formation, synthesis, and genotoxicity of the *N*-hydroxy derivative of the food mutagen 2-amino-1-methyl-6-phenylimidazo[4,5-*b*]pyridine (PhIP). *Mutagenesis* **6**, 93–98.

(16) Buonarati, M. H., Turteltaub, K. W., Shen, N. H., and Felton, J. S. (1990) Role of sulfation and acetylation in the activation of 2-hydroxyamino-1-methyl-6-phenylimidazo[4,5-*b*]pyridine to intermediates which bind DNA. *Mutat. Res.* **245**, 185–190.

(17) Takayama, K., Yamashita, K., Wakabayashi, K., Sugimura, T., and Nagao, M. (1989) DNA modification by 2-amino-1-methyl-6-phenylimidazo[4,5-*b*]pyridine in rats. *Jpn. J. Cancer Res.* **80**, 1145–1148.

(18) Snyderwine, E. G., Schut, H. A. J., Adamson, R. H., Thorgeirsson, U. P., and Thorgeirsson, S. S. (1992) Metabolic activation and genotoxicity of heterocyclic amines. *Cancer Res. (Suppl.)* **52**, 2099s–2102s.

(19) Turteltaub, K. W., Frantz, C. E., Creek, M. R., Vogel, J. S., Shen, N., Fultz, E. (1993) DNA adducts in model systems and humans. *J. Cell. Biochem. (Suppl.)* **17F**, 138–148.

(20) Snyderwine, E. G., Davis, C. D., Nouso, K., Roller, P. P., and Schut, H. A. J. (1993) ^{32}P-Postlabeling analysis of IQ, MeIQx, and PhIP adducts formed *in vitro* in DNA and polynucleotides and found *in vivo* in hepatic DNA from IQ-, MeIQx- and PhIP-treated monkeys. *Carcinogenesis* **14**, 1389–1395.

(21) Nagaoka, H., Wakabayashi, K., Kim, S.-B., Kim, I.-S., Tanaka, Y., Ochiai, M., Tada, A., Nukaya, H., Sugimura, T., and Nagao, M. (1992) Adduct formation at C-8 of guanine on *in vitro* reaction of the ultimate form of 2-amino-1-methyl-6-phenylimidazo[4,5-*b*]pyridine with 2′-deoxyguanosine and its phosphate esters. *Jpn. J. Cancer Res.* **83**, 1025–1029.

(22) Lin, D., Kaderlik, K. R., Turesky, R. J., Miller, D. W., Lay, J. O., Jr., and Kadlubar, F. F. (1992) Identification of *N*-(deoxyguanosin-8-yl)-2-amino-1-methyl-6-phenylimidazo[4,5-*b*]pyridine as the major adduct formed by the food-borne carcinogen, 2-amino-1-methyl-6-phenylimidazo[4,5-*b*]pyridine, with DNA. *Chem. Res. Toxicol.* **5**, 691–697.

(23) Frandsen, H., Grivas, S., Andersson, R., Dragsted, L., and Larsen, J. C. (1992) Reaction of the N^2-acetoxy derivative of 2-amino-1-methyl-6-phenylimidazo[4,5-*b*]pyridine (PhIP) with 2′-deoxyguanosine and DNA. Synthesis and identification of N^2-(2′-deoxyguanosin-8-yl)-PhIP. *Carcinogenesis* **13**, 629–635.

(24) Turesky, R. J., Rossi, S. C., Welti, D. H., Lay, J. O., Jr., and Kadlubar, F. F. (1992) Characterization of DNA adducts formed *in vitro* by reaction of *N*-hydroxy-2-amino-3-methylimidazo[4,5-*f*]quinoline and *N*-hydroxy-2-amino-3,8-dimethylimidazo[4,5-*f*]-quinoxaline at the C-8 and N^2 atoms of guanine. *Chem. Res. Toxicol.* **5**, 479–490.

(25) Turesky, R. J., and Markovic, J. (1994) DNA adduct formation of the food carcinogen 2-amino-3-methylimidazo[4,5-*f*]quinoline at the C-8 and N^2 atoms of guanine. *Chem. Res. Toxicol.* **7**, 752–761.

(26) Carothers, A. M., Yuan, W., Hingerty, B. E., Broyde, S., Grunberger, D., and Snyderwine, E. G. (1994) Mutation and repair induced by the carcinogen 2-(hydroxyamino)-1-methyl-6-phenylimidazo[4,5-*b*]pyridine (*N*-OH-PhIP) in the dihydrofolate reductase gene of Chinese hamster ovary cells and conformational modeling of the dG-C8-PhIP adduct in DNA. *Chem. Res. Toxicol.* **7**, 209–218.

(27) Reddy, M. V., and Randerath, K. (1986) Nuclease P1-mediated enhancement of sensitivity of ^{32}P-Postlabeling test for structurally diverse DNA adducts. *Carcinogenesis* **7**, 1543–1551.

(28) Turteltaub, K. W., Watkins, B. E., Vanderlaan, M., and Felton, J. S. (1990) Role of metabolism on the DNA binding of MeIQx in mice and bacteria. *Carcinogenesis* **11**, 43–49.

(29) Marsch, G. A., Ward, R. L., Colvin, M., and Turteltaub, K. W. (1994) Noncovalent DNA groove-binding by 2-amino-1-methyl-6-phenylimidazo[4,5-*b*]pyridine. *Nucleic Acids Res.* **22**, 5408–5415.

(30) Becker, R. S. (1969) *Theory and Interpretation of Fluorescence and Phosphorescence*, Chapter 8, pp 87–88, Wiley Interscience, New York, NY.

(31) De Schruyer, F. C., and De Keukeleire, D. (1991) Fluorescence spectroscopy: an introduction. In *Luminescence Techniques in Chemical and Biochemical Analysis* (Baeyens, W. R. G., De Keukeleire, D., and Korkidis, K., Eds.) pp 13–19, Marcel Dekker, New York, NY.

(32) Cooper, R. S., Jankowiak, R., and Small, G. J. (1991) Bioanalytical applications of fluorescence line-narrowing spectroscopy. In *Luminescence Techniques in Chemical and Biochemical Analysis* (Baeyens, W. R. G., De Keukeleire, D., and Korkidis, K., Eds.) p 203, Marcel Dekker, New York, NY.

(33) Marsch, G. A., Jankowiak, R., and Small, G. J. (1992) Evidence of involvement of multiple sites of metabolism in the *in vivo* covalent binding of dibenzo[*a*,*h*,]pyrene to DNA. *Chem. Res. Toxicol.* **5**, 765–772.

(34) Geacintov, N. E. (1987) Principles and applications of fluorescence techniques in biophysical chemistry. *Photochem. Photobiol.* **45**, 547–553.

(35) Undeman, O., Lycksell, P.-O., Gräslund, A., Astlind, T., Ehrenberg, A., Jernström, B., Tjerneld, F., and Nordén, B. (1983) Covalent complexes of DNA and two stereoisomers of benzo[*a*]-pyrene 7,8-dihydrodiol-9,10-epoxide studied by fluorescence and linear dichroism. *Cancer Res.* **43**, 1851–1860.

(36) Geacintov, N. E. (1985) Mechanisms in interaction of polycyclic aromatic diol epoxides with DNA and structures of the adducts. In *Polycyclic Hydrocarbons and Carcinogenesis* (Harvey, R. G., Ed.) pp 107–124, American Chemical Society, Washington, DC.

(37) Dattagupta, N., and Crothers, D. M. (1981) Solution structural studies of the Ag(I)-DNA complex. *Nucleic Acids Res.* **9**, 2971–2985.

(38) Undeman, O., Sahlin, M., Gräslund, A., Ehrenberg, A., Dock, L., and Jernström, B. (1980) Fluorescence study of (±)-*trans*-7,8-dihydro-benzo[*a*]pyrene metabolism *in vitro* and binding to DNA. *Biochem. Biophys. Res. Commun.* **94**, 458–465.

(39) van Houte, L. P. A., van Grondelle, R., Retèl, J., Westra, J. G., Zinger, D., Sutherland, J. C., Kim, S. K., and Geacintov, N. E. (1989) Excited state properties of the N-(deoxyguanosin-8-yl)-2-aminofluorene adducts. *Photochem. Photobiol.* **49**, 387–394.

(40) Geacintov, N. E., Zinger, D., Ibanez, V., Santella, R., Grunberger, D., and Harvey, R. G. (1987) Properties of covalent benzo[*a*]pyrene diol epoxide–DNA adducts investigated by fluorescence techniques. *Carcinogenesis* **7**, 925–935.

(41) Kadlubar, F. F., Melchior, W. B., Jr., Flammang, T. J., Gagliano, A. G., Yoshida, H., and Geacintov, N. E. (1981) Structural consequences of modification of the oxygen atom of guanine in DNA by the carcinogen *N*-hydroxy-1-naphthylamine. *Cancer Res.* **41**, 2168–2174.

(42) Prusik, T., Geacintov, N. E., Tobiasz, C., Ivanovic, V., and Weinstein, I. B. (1979) Fluorescence study of the physico-chemical properties of a benzo[*a*]pyrene 7,8-dihydrodiol 9,10-oxide derivative bound covalently to DNA. *Photochem. Photobiol.* **29**, 223–232.

(43) Kim, S. G., Brenner, H. C., Soh, B. J., and Geacintov, N. E. (1989) Fluorescence spectroscopy of benzo[*a*]pyrene diol epoxide–DNA adducts. Conformation-specific emission spectra. *Photochem. Photobiol.* **50**, 327–337.

(44) Jankowiak, R., Lu, P., Small, G. J., and Geacintov, N. E. (1990) Laser-spectroscopic studies of DNA adduct structure types from enantiomeric diol epoxides of benzo[*a*]pyrene. *Chem. Res. Toxicol.* **3**, 39–46.

(45) Lu, P., Jeong, H., Jankowiak, R., Small, G. J., Kim, S. K., Cosman, M., and Geacintov, N. E. (1991) Comparative laser spectroscopic study of DNA and polynucleotide adducts from the (+)-*anti*-diol epoxide of benzo[*a*]pyrene. *Chem. Res. Toxicol.* **4**, 58–69.

(46) Marsch, G. A., Jankowiak, R., Suh, M., and Small, G. J. (1994) Sequence dependence of benzo[*a*]pyrene diol epoxide–DNA adduct conformer distribution: a study by laser-induced fluorescence/polyacrylamide gel electrophoresis. *Chem. Res. Toxicol.* **7**, 98–109.

(47) Norman, D., Abuaf, P., Hingerty, B. E., Live, D., Grunberger, D., Broyde, S., and Patel, D. J. (1989) NMR and computational characterization of the *N*-(deoxyguanosin-8-yl)aminofluorene adduct [(AF)G] opposite adenosine in DNA: (AF)G[syn]·A[anti] pair formation and its pH dependence. *Biochemistry* **28**, 7462–7476.

(48) Hertzog, P. J., Lindsay-Smith, J. R., and Garner, R. C. (1982) Characterization of the imidazole ring-opened forms of *trans*-8,9-dihydro-8-(7-guanyl)-9-hydroxy aflatoxin B_1. *Carcinogenesis* **3**, 723–725.

(49) Pfau, W., Brockstedt, U., Söhren, K.-D., and Marquardt, H. (1994) ^{32}P-Postlabelling analysis of DNA adducts formed by food-derived heterocyclic amines: evidence for incomplete hydrolysis and a procedure for adduct pattern simplification. *Carcinogenesis* **15**, 877–882.

(50) Reddy, A. P., Pruess-Schwartz, D., and Marnett, L. J. (1992) Separation of (+)-*syn*- and (−)-*anti*-benzo[*a*]pyrene dihydrodiol epoxide–DNA adducts in ^{32}P-postlabeling analysis. *Chem. Res. Toxicol.* **5**, 19–25.

(51) Canella, K. A., Peltonen, K., Yagi, H., Jerina, D. M., and Dipple, A. (1992) Identification of individual benzo[*c*]phenanthrene dihydrodiol epoxide–DNA adducts by the ^{32}P-postlabeling assay. *Chem. Res. Toxicol.* **5**, 685–690.

(52) Margulis, L., Pluzhnikov, P. F., Mao, B., Kuzmin, V. A., Chang, Y. J., Scott, T. W., and Geacintov, N. E. (1991) Photoinduced electron transfer in a covalent benzo[*a*]pyrene diol epoxide–2′-deoxyguanosine complex. *Chem. Phys. Lett.* **187**, 597–603.

(53) Yamamoto, J., Subramaniam, R., Wolfe, A. R., and Meehan, T. (1990) The formation of covalent adducts between benzo[*a*]pyrene diol epoxide and RNA: structural analysis by mass spectrometry. *Biochemistry* **29**, 3966–3972.

(54) Zhao, R., Liu, T.-M., Kim, S. K., MacLeod, M. C., and Geacintov, N. E. (1992) Identification and quantitative detection of isomeric benzo[*a*]pyrene diol epoxide-DNA adducts by low-temperature conventional fluorescence methods. *Carcinogenesis* **13**, 1817–1824.

(55) Chen, J., MacLeod, M. C., Zhao, R., and Geacintov, N. E. (1993) Fluorescence HPLC methods for detecting benzo[*a*]pyrene-7,8-dihydrodiol 9,10-oxide-deoxyadenosine adducts in enzyme-digests of modified DNA: improved sensitivity. *Carcinogenesis* **14**, 1049–1051.

(56) Geacintov, N. E., Zhao, R., Kuzmin, V. A., Kim, S. K., and Pecora, L. J. (1993) Mechanisms of quenching of the fluorescence of a benzo[*a*]pyrene tetraol metabolite model compound by 2′-deoxynucleotides. *Photochem. Photobiol.* **58**, 185–194.

TX950020S